Hindawi
International Transactions on Electrical Energy Systems
Volume 2022, Article ID 6587478, 10 pages
https://doi.org/10.1155/2022/6587478

Research Article

Robust Optimal Scheduling of EHG-IES Based on Uncertainty of Wind Power and PV Output

Minsheng Yang,[1,2] **Jianying Li**,[1,2] **Jian Sun**,[1,2] **Jiazhu Xu**,[3] **and Jianqi Li**[1,2]

[1]*College of Computer and Electrical Engineering, Hunan University of Arts and Science, Changde 415000, China*
[2]*Key Laboratory of Hunan Province for Control Technology of Distributed Electric Propulsion Air Vehicle, Changde 415000, China*
[3]*College of Electrical and Information Engineering, Hunan University, Changsha 410082, China*

Correspondence should be addressed to Minsheng Yang; yms1234@163.com

Received 10 October 2021; Revised 30 November 2021; Accepted 15 December 2021; Published 31 January 2022

Academic Editor: Sujin Bureerat

The Electricity-Heat-Gas Integrated Energy System (EHG-IES) is important for achieving carbon neutrality. However, the uncertainty of wind power and photovoltaic (PV) output has a large impact on EHG-IES scheduling optimization. In order to solve this problem, a robust scheduling optimization method considering the uncertainty of wind power and PV output and the coupling relationship of each device in EHG-IES is proposed. In the proposed optimization method, the uncertainty of wind power and PV output is described by an additive maximum uncertainty set. Then, the day-ahead scheduling optimization model is proposed based on the coupling relationship of each equipment and electric vehicle (EV) traveling demand. Also, the proposed model is introduced in detail. The simulation is verified by a park calculation example. The economy and accuracy of the proposed method in this paper are verified by comparing the robust optimization results under different uncertainties with stochastic optimization. For robust parameters of 20% and 10%, the economic cost is 1.016% and 1.041% lower than that of the stochastic optimization. Meanwhile, the proposed method can improve the economy of the EHG-IES and realize the economic and safe operation of the EHG-IES under the consideration of EVs and heating storage equipment.

1. Introduction

As the Energy Internet (EI) flourishes globally, renewable energy and its equipment technologies have been further developed. The Electricity-Heat-Gas (EHG) Integrated Energy System (EHG-IES) can improve energy utilization and reduce carbon emissions to achieve sustainable development [1, 2].

The EHG-IES scheduling optimization problem has been studied by a large number of local and abroad scholars. Multienergy sources are considered in an EHG-IES microgrid system and analyzed the operation under different wind power penetration rates [3, 4]. Although multienergy sources in EHG are analyzed, the uncertainty of renewable energy source (RES) output is not considered. Based on this, the scenario approach is used to represent the uncertainty of RES generation in IES optimization [5–8]. In [7], scenarios using Monte Carlo (MC) simulations were generated to characterize the uncertainty of RES output, while the Latin hypercube sampling is addressed in [8]. Also, the optimal strategy is solved under the constraints of three networks: electric, gas, and heat. Scenario-based stochastic optimization (SO) is used to deal with uncertainties associated with electric loads, wind power, and electricity prices. Also, an optimal stochastic dispatch problem integrating power to gas (P2G) storage, combined heat and power (CHP) units, wind power, boilers, power storage, and heating storage for energy hub (EH) is proposed [9, 10]. For the uncertainty of RES output, many scenarios are generated with probability density function (PDF) for simulation. The deterministic scenarios are reduced to select scenarios that can represent the uncertainty. However, the existing studies show that the

RES output is highly related to the weather and environment and does not exactly obey the PDF. Also, there are difficulties in selecting representative scenarios from many deterministic scenarios to be involved in scheduling. In the optimal operation of the IES, the analysis is performed only for the uncertainty of RES output.

To overcome some of the shortcomings of the SO, some scholars have combined SO with robust optimization. In [11], the uncertainty of RES and load of capacity planning is represented in EH by a fuzzy PDF. However, the method requires moderate uncertainty information. A robust day-ahead scheduling model is considered using chance constraints to represent the stochastic characteristics of RES generation and loads [12]. The optimal operation model of the smart multienergy districts containing uncertainty of energy demand is developed and the energy storage battery is taken into account in the model in [13]. In [14], a stochastic robust optimization operation model based on integrated demand response is presented, focusing on the coordinated complementarity of multiple energy sources. Therefore, an energy planning model for distribution systems considering different demands and energy carriers is proposed. Also, the role of electric, heating, and cooling energy storage is analyzed; however, the uncertainty of RES output is not considered [15]. The study in [16] focuses on the modeling of biogas participation in multienergy management. The study in [17] addresses the energy management problem considering the equipment coupling relationship of RES combined heat and power supply and heat storage (HS). But, the abovementioned literature focuses on improving the shortcomings of SO, and the abovementioned studies do not take into account the impact of energy storage, and the improved methods also require a large amount of uncertain information.

Considering the uncertainty of RES output, there are few studies on the coupled scheduling between different energy sources. In [18], the role of HS in the optimal expansion for multienergy systems is analyzed. Also, the work in [19, 20] develops a model of the thermoelectric components in CHP to accurately respond to thermoelectric interactions and improved efficiency and stability. The work in [21] introduces a microgrid scheduling model containing different energy sources under different scenarios to enhance energy scheduling. However, the impact of multiple energy sources' uncertainty is not considered in [22]. The P2G, capture device, and CHP are considered as a whole to participate in the scheduling problem [23]. The uncertainty of RES output has an important impact on EHG-IES operation. A robust optimization model including EVs is established in the energy management system, but the impact of multiple storage devices is not taken into account [10]. However, the role of the volatility of electric vehicles (EVs) and RES output in scheduling optimization is not highlighted. Also, with the development of EVs, the impact of EVs cannot be ignored; however, no analysis is performed in the existing studies.

From the abovementioned analysis, it can be concluded that existing studies have mainly modeled and analyzed the complementary characteristics of RES in IES or have considered only the uncertainty of RES output separately. There are two problems that need to be solved: (1) The role of different energy storage devices under the uncertainty of RES output has not been analyzed in EHG-IES. (2) The travel demand for EVs and heat conversion functions are not considered in the day-ahead scheduling model.

To solve the problems, a day-ahead robust optimization model that simultaneously considers the uncertainty of RES output and different energy storage devices is proposed. The main work of this paper can be summarized as follows:

(1) Based on the uncertainty of RES output by using the uncertainty set containing addition, the robust day-ahead scheduling model of EHG-IES is established by considering the coupling characteristics between different energy storage devices.

(2) The impact of EVs and HS is analyzed by considering the EVs travel demand and the heat conversion functions in the model. The different scenarios under different degrees of uncertainty are compared and analyzed in terms of economy and robustness with SO.

(3) An example validation of a park case is carried out. The model is validated by the actual example. The scenarios with different robust parameters are analyzed and discussed to verify the accuracy and economy of the strategy in this paper.

This paper is structured as follows: Section 2 focuses on the analysis of the EHG-IES structure. Section 3 introduces the EHG-IES day-ahead scheduling model and the robust set. Section 4 analyzes the actual arithmetic cases. Section 5 is the conclusion.

2. EHG-IES Structural Analysis

In the EHG-IES structure, the main structure is shown in Figure 1, focusing on a system that includes two types of energy storage: EVs and Heat Storage (HS). Photovoltaic (PV) and wind power output is integrated into the power network. Also, EVs are charged when there is excess RES output, and electricity prices are low to improve the utilization of energy. When there is a shortage of energy, EVs are discharged and electricity is purchased from the upper grid to meet the electrical load. Natural gas is fed into the electric and heating networks through microgas turbines (MT) and gas boilers (GB), respectively. The MT provides the required electricity to the customer and is capable of recovering the high-temperature waste heat gas from operation through a waste heat boiler (WHB) and producing heat through a heat exchanger (HE). The heating from the waste heat recovery unit and the GB is supplied to the heating load through the HE, or the heating load can be supplied by the electric boiler (EB) when the electricity price is low. If the flue gas waste heat cannot meet the heating load demand of the customer, the GB will supply the heat to the customer. When HE and HS cannot meet the heating power balance, GB, EB converts electrical energy into heat to meet it. HS, like EVs, stores heating energy when the heating energy cost is low and performs heating energy release when the heating energy

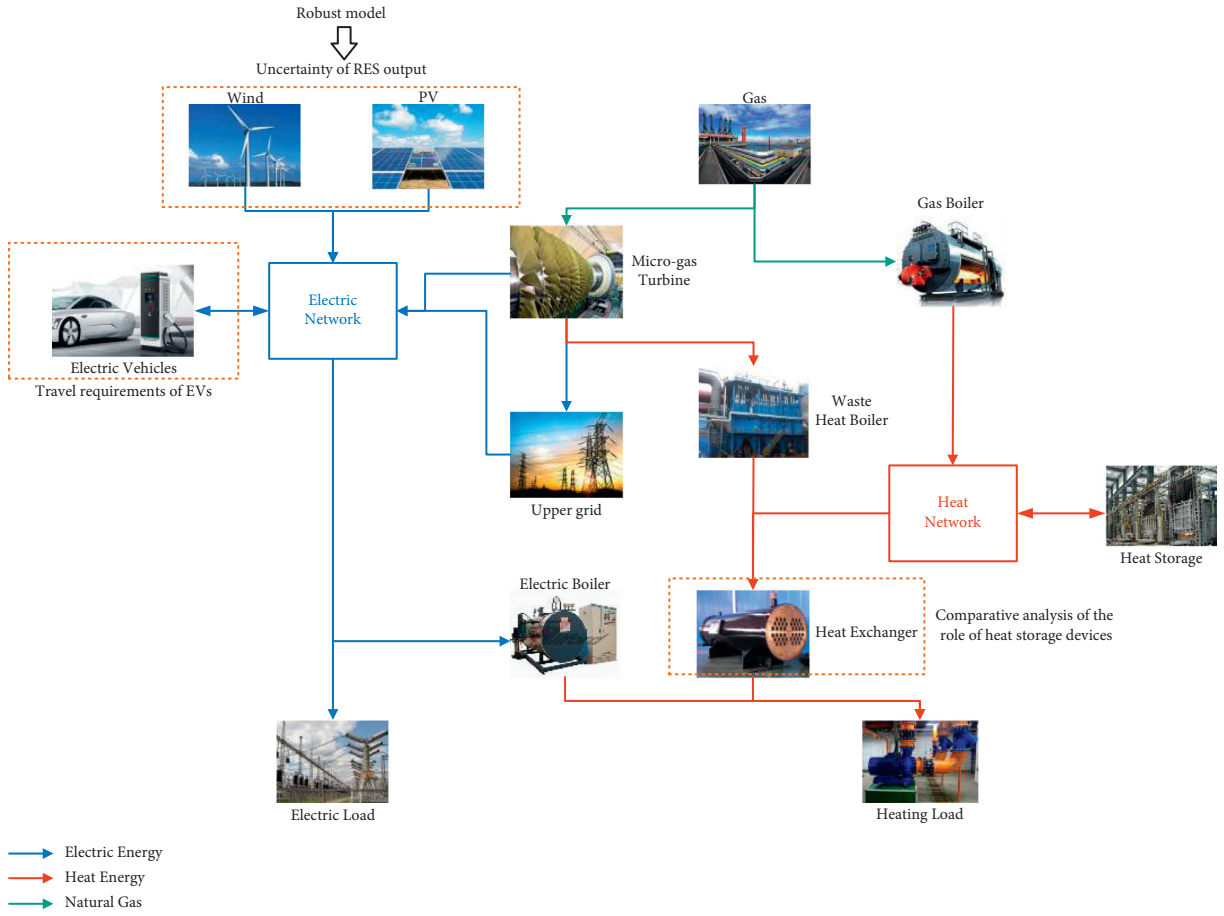

Figure 1: EHG-IES structure.

cost is high [24]. PV and wind power carry out the power supply, and if there is still a shortage of electrical load, it can be supplemented by purchasing power from the upper grid. EVs and energy storage devices such as HS will reasonably realize the storage and release of energy according to the developed operation scheme and, thus, improve the matching of supply and demand of the systems.

3. EHG-IES Optimal Scheduling Model

A robust optimal scheduling model is established for the uncertainty of wind power and PV output. Also, the coupling relationship between each device, mainly the characteristics of both EVs and HS included in EHG-IES, is also taken into consideration.

3.1. Objective Function of the Scheduling Model. The objective function is to minimize the system operating cost, including the cost of electricity purchased from the upper grid, and the operating cost, as shown in the following equation:

$$\min F = \min\left(F_{\text{grid}} + F_{\text{op}}\right), \tag{1}$$

where the cost of purchasing electricity from the upper grid F_{grid} is

$$F_{\text{grid}} = \sum_{t=1}^{T} C_{\text{grid},t} P_{\text{grid},t}. \tag{2}$$

Operating costs F_{op}:

$$F_{\text{op}} = \sum_{t=1}^{T} C_{\text{gas},t}\left(\frac{\phi_{\text{MT}} P_{\text{MT},t} + \varphi_{\text{MT}} I_{\text{MT},t} + F_{\text{GB},t}}{L_{\text{NG}}}\right), \tag{3}$$

where T indicates the scheduling time. $C_{\text{grid},t}$ and $C_{\text{gas},t}$ denote the price of electricity and natural gas purchased from the upper grid. $P_{\text{MT},t}$ denotes the output power of MT at time t. $P_{\text{grid},t}$ is grid-purchased electricity. ϕ_{MT} and φ_{MT} represent the fuel factor of MT. $F_{\text{GB},t}$ is the GB cost function [25]. $I_{\text{MT,t}}$ is the MT start/stop 0-1 flag variable. L_{NG} is the low calorific value of natural gas.

3.2. Constraints. EHG-IES needs to meet the electric, heating, and gas power balance constraints and various equipment constraints.

3.2.1. Power Balance Constraints. The various types of energy sources in EHG-IES need to meet different energy balance constraints.

Electrical power balance:

$$P_{w,t} + P_{\mathrm{pv},t} + P_{\mathrm{MT},t} + P_{\mathrm{grid},t} = P_{\mathrm{load},t} + P_{\mathrm{EB},t} + P_{\mathrm{escha},t} - P_{\mathrm{esdis},t}. \tag{4}$$

Heat power balance:

$$H_{\mathrm{MT},t} + H_{\mathrm{EB},t} + H_{\mathrm{GB},t} = H_{\mathrm{load},t} + H_{\mathrm{hschr},t} - H_{\mathrm{hsdis},t}. \tag{5}$$

Gas network balance:

$$V_{\mathrm{gas},t} = V_{\mathrm{MT},t} + V_{\mathrm{GB},t}, \tag{6}$$

where $P_{w,t}, P_{\mathrm{pv},t}$ denote the wind power and PV output at time t. $P_{\mathrm{load},t}, P_{\mathrm{EB},t}, P_{\mathrm{escha},t}, P_{\mathrm{esdis},t}$ mean electric load power, power of EB, and charging and discharging power of EVs. $H_{\mathrm{MT},t}, H_{\mathrm{EB},t}, H_{\mathrm{GB},t}$ indicate the heat power output of MT, EB, and GB. $H_{\mathrm{load},t}, H_{\mathrm{hschr},t}, H_{\mathrm{hsdis},t}$ indicate the heating load power, heat charging power of HS, and heating discharging power of HS. $V_{\mathrm{gas},t}$ represents the output of gas from the gas grid. $V_{\mathrm{MT},t}$ denotes the natural gas input of MT at time t. $V_{\mathrm{GB},t}$ is the natural gas input of GB at time t.

3.2.2. Equipment Constraints. The MT is the core of the EHG-IES system, which converts primary natural gas into electricity and generates waste heat for cooling and heating. MT generation efficiency and waste heat efficiency are different at different load rates and have variable operating characteristics [26].

During MT operation, the discharged high-temperature waste heat flue gas is recovered by WHB and then passed through HE for heat production. The characteristic model of MT is

$$\begin{aligned} G_{\mathrm{MT},t} &= \frac{P_{\mathrm{MT},t}\left(1 - \eta_{\mathrm{MT}} - \eta_L\right)}{\eta_{\mathrm{MT}}}, \\ H_{\mathrm{MT},t} &= G_{\mathrm{MT},t} C_{\mathrm{OP},h} \eta_h, \end{aligned} \tag{7}$$

where $G_{\mathrm{MT},t}$ is the waste heat of MT's exhaust. $\eta_{\mathrm{MT}}, \eta_L$ represent the power generation efficiency of MT and heat dissipation self-loss coefficient. $H_{\mathrm{MT},t}$ is the heat production of MT. $C_{\mathrm{OP},h}$ and η_h are the heat production coefficient and flue gas recovery rate.

The characteristics of MT make its output force be varied only within a certain range. The MT also needs to meet its upper and lower output limits and climbing constraints:

$$\begin{aligned} P_{\mathrm{MT,min}} \le P_{\mathrm{MT},t} \le P_{\mathrm{MT,max}}, \\ P_{\mathrm{MT},t} - P_{\mathrm{MT},t-1} \le P_{\mathrm{MT,up}}, \\ P_{\mathrm{MT},t-1} - P_{\mathrm{MT},t} \le P_{\mathrm{MT,down}}, \end{aligned} \tag{8}$$

where $P_{\mathrm{MT,min}}, P_{\mathrm{MT,max}}$ are the lower and upper output limits of MT. $P_{\mathrm{MT,up}}$ and $P_{\mathrm{MT,down}}$ represent the upper and lower MT climbing limits.

EB mainly uses electrical energy as the energy source. Heating energy is generated by electrical resistance or electromagnetic induction. Also, EB heats the organic heat carrier to a certain temperature or pressure through its heat exchange part and then outputs heat energy to the outside. EB converts electricity into heat to meet demand during low electricity prices [27].

$$\begin{aligned} H_{\mathrm{EB},t} &= P_{\mathrm{EB},t}\eta_{\mathrm{EB}}, \\ 0 \le P_{\mathrm{EB},t} &\le P_{\mathrm{EB,max}}, \end{aligned} \tag{9}$$

where $H_{\mathrm{EB},t}$ indicates the output heat power of EB. η_{EB} denotes the EB efficiency factor.

When HE, HS, and EB cannot meet heat power balance, it is achieved by GB.

$$\begin{aligned} H_{\mathrm{GB},t} &= V_{\mathrm{GB},t}\eta_{\mathrm{GB}}, \\ H_{\mathrm{GB,min}} \le H_{\mathrm{GB},t} &\le H_{\mathrm{GB,max}}, \end{aligned} \tag{10}$$

where $H_{\mathrm{GB},t}$ indicates the heat power output of GB. $V_{\mathrm{GB},t}$ is the natural gas consumption of GB. η_{GB} denotes the efficiency factor.

EVs are a high-quality energy storage resource. EVs are discharged when there is a shortage of electricity and charged when there is a surplus of electricity and electricity prices are low. EVs need to satisfy the state of charge (SOC) and its characteristic constraints. Considering the travel demand of EVs, charging and discharging are not available at 7:00 and 18:00 [28].

$$\begin{aligned} I_{\mathrm{eschr},t}P_{\mathrm{eschr,min}} \le P_{\mathrm{eschr},t} \le I_{\mathrm{eschr},t}P_{\mathrm{eschr,max}}, \\ I_{\mathrm{esdis},t}P_{\mathrm{esdis,min}} \le P_{\mathrm{esdis},t} \le I_{\mathrm{esdis},t}P_{\mathrm{esdis,max}}, \\ \mathrm{SOC_{min}} \le \mathrm{SOC}_t \le \mathrm{SOC_{max}}, \\ \mathrm{SOC}_t = \mathrm{SOC}_{t-1} + \left(\eta_{\mathrm{escha}}P_{\mathrm{eschr},t} - \frac{\eta_{\mathrm{esdis}}P_{\mathrm{esdis},t}}{\eta_{\mathrm{esdis}}}\right), \\ 0 \le I_{\mathrm{eschr},t} + I_{\mathrm{esdis},t} \le 1, \\ I_{\mathrm{eschr},7} + I_{\mathrm{esdis},7} = 0, \\ I_{\mathrm{eschr},18} + I_{\mathrm{esdis},18} = 0, \end{aligned} \tag{11}$$

where $P_{\mathrm{eschr,min}}, P_{\mathrm{eschr,max}}$ are the min and max charging power of EVs. $P_{\mathrm{esdis,min}}, P_{\mathrm{esdis,max}}$ are the min and max discharging power of EVs. $\mathrm{SOC_{min}}, \mathrm{SOC_{max}}$ are the minimum and maximum value of SOC. $\eta_{\mathrm{escha}}, \eta_{\mathrm{esdis}}$ are EVs' charging efficiency and discharging efficiency. $I_{\mathrm{eschr},t}, I_{\mathrm{esdis},t}$ indicate EVs' status flag variable.

HS stores heat energy when there is too much in the system and releases it when there is not enough or when the price of heat is high, thus gaining revenue and improving the economy. HS needs to meet its operational characteristics:

$$\begin{aligned} E_{\mathrm{hs},t} = E_{\mathrm{hs},t-1}\left(1 - \gamma_h\right) + \left(\eta_{\mathrm{hschr}}H_{\mathrm{hschr},t} - \frac{H_{\mathrm{hsdis},t}}{\eta_{\mathrm{hsdis}}}\right), \\ E_{\mathrm{hs,min}} \le E_{\mathrm{hs},t} \le E_{\mathrm{hs,max}}, \\ U_{\mathrm{hschr},t}H_{\mathrm{hschr,min}} \le H_{\mathrm{hschr},t} \le U_{\mathrm{hschr},t}H_{\mathrm{hschr,max}}, \\ U_{\mathrm{hsdis},t}H_{\mathrm{hsdis,min}} \le H_{\mathrm{hsdis},t} \le U_{\mathrm{hsdis},t}H_{\mathrm{hsdis,max}}, \\ 0 \le U_{\mathrm{hschr},t} + U_{\mathrm{hsdis},t} \le 1, \end{aligned} \tag{12}$$

where $E_{\mathrm{hs},t}$ represents the heat energy stored in the HS. γ_h is the self-loss coefficient of HS. $H_{\mathrm{hschr},t}$, $H_{\mathrm{hsdis},t}$ indicate heat charge power and discharge power. $U_{\mathrm{hschr},t}$, $U_{\mathrm{hsdis},t}$ are charging and discharging flag variables.

When the system is in operation, it needs to interact with the upper grid, except for the distributed energy sources and EVs and HS in the system for energy supply. When interacting with the upper grid, upper and lower bound constraints need to be satisfied:

$$P_{\mathrm{grid,min}} \le P_{\mathrm{grid},t} \le P_{\mathrm{grid,max}}, \tag{13}$$

where $P_{\mathrm{grid,min}}, P_{\mathrm{grid,max}}$ are the lower and upper limits of power purchased from the upper grid.

Positive spinning reserve capacity constraint:

In case of system load overload, the upper grid and MT can provide spinning reserve capacity for the system.

$$\begin{aligned} &P_{\mathrm{MT,max}} + P_{\mathrm{esdis},t} - P_{\mathrm{escha},t} + P_{\mathrm{grid},t} + P_{w,t} + P_{\mathrm{pv},t} \\ &\ge P_{\mathrm{load},t}\,(1 + \mathrm{RL}\%) + P_{\mathrm{EB},t}. \end{aligned} \tag{14}$$

Negative spinning reserve capacity constraint:

$$\begin{aligned} &P_{\mathrm{MT,min}} + P_{\mathrm{esdis},t} - P_{\mathrm{escha},t} + P_{\mathrm{grid,min}} + P_{w,t} + P_{\mathrm{pv},t} \\ &\le P_{\mathrm{load},t}\,(1 - \mathrm{RL}\%) + P_{\mathrm{EB},t}. \end{aligned} \tag{15}$$

3.3. Robust Model. The general model of EHG-IES optimal dispatch considering the uncertainty of renewable energy output in general is

$$\begin{aligned} &\min_{x \in X} M^T x + N^T y, \\ &\text{s.t. } Ax + By + C\omega \le (\ge / =) D, \end{aligned} \tag{16}$$

where x and y are decision variables. w is a random variable, which is the uncertainty of renewable energy output. M, N, and A–C are known coefficient matrices/vectors, D denotes the known parameter, and X is the definition domain of decision variable x. When the renewable energy output changes, the EHG-IES is operated safely and stably by adjusting the unit output and the rest of the equipment to ensure the power balance and other constraints.

$$\begin{aligned} &\max_{\omega} \min_{x,y} Mx + N^T y, \\ &\text{s.t. } Ax + By + C\omega \le (\ge / =) D. \end{aligned} \tag{17}$$

To realize the system scheduling strategy generation under the uncertainty-containing output, the above-mentioned robust optimization model is converted into a max-min model using pairwise theory, in which the uncertainty of renewable energy output is most notably represented by an uncertainty set to find the result in the extreme scenario.

For the uncertainty of wind power and PV output in EHG-IES, equations (14) and (15) need to be converted.

$$\begin{aligned} p = \Big\{ & P_{\mathrm{res},t} = \overline{P_{\mathrm{res},t}} + \gamma_{\mathrm{res},t} \Delta P_{\mathrm{res},t}, \forall \mathrm{res}, t: \left\| \gamma_{\mathrm{res},t} \right\|_{\infty} \\ & \le 1, \left\| \gamma_{\mathrm{res},t} \right\|_1 \le \Gamma_R \Big\}, \\ \left\| \gamma_{\mathrm{res},t} \right\|_{\infty} &= \max \left| \gamma_{\mathrm{res},t} \right|, \left\| \gamma_{\mathrm{res},t} \right\|_1 = \sum \left| \gamma_{\mathrm{res},t} \right|, \end{aligned} \tag{18}$$

where $\gamma_{\mathrm{res},t}$ indicates the deviation factor of wind power output. $\|\gamma_{\mathrm{res},t}\|_{\infty}$ and $\|\gamma_{\mathrm{res},t}\|_1$ are the infinite norm and 1-norm. Γ_R is the robustness parameter of the wind power output, which is mainly used to adjust the robustness of the system.

After constructing the uncertainty set, the conversion of equations (14) and (15) in the constraints is performed using the dual conversion, which is as follows:

$$\begin{aligned} &- \sum x_{\mathrm{res},t} \overline{P_{\mathrm{res},t}} + \sum y_{\mathrm{res},t} \overline{P_{\mathrm{res},t}} - \sum \alpha_{\mathrm{res},t} - \Gamma_R \beta_t \\ &\ge P_{\mathrm{load},t}\,(1 + \mathrm{RL}\%) + P_{\mathrm{EB},t} - P_{\mathrm{MT,max}} - P_{\mathrm{esdis},t} \\ &\quad + P_{\mathrm{escha},t} - P_{\mathrm{grid},t}, \\ &\text{s.t.} \begin{cases} -x_{\mathrm{res},t} + y_{\mathrm{res},t} \le 1, \\ \Delta P_{\mathrm{res},t} \left(x_{\mathrm{res},t} + y_{\mathrm{res},t} \right) - \alpha_{\mathrm{res},t} - \beta_t \le 0, \\ x_{\mathrm{res},t}, y_{\mathrm{res},t}, \alpha_{\mathrm{res},t}, \beta_t \ge 0, \end{cases} \\ &\sum \mu_{\mathrm{res},t} \overline{P_{\mathrm{res},t}} - \sum \nu_{\mathrm{res},t} \overline{P_{\mathrm{res},t}} + \sum \varsigma_{\mathrm{res},t} + \Gamma_R \xi_t \\ &\le P_{\mathrm{load},t}\,(1 - \mathrm{RL}\%) + P_{\mathrm{EB},t} - P_{\mathrm{MT,min}} - P_{\mathrm{esdis},t} + P_{\mathrm{escha},t} \\ &\quad - P_{\mathrm{grid,min}}, \\ &\text{s.t.} \begin{cases} \mu_{\mathrm{res},t} - \nu_{\mathrm{res},t} \ge 1, \\ -\Delta P_{\mathrm{res},t} \left(\mu_{\mathrm{res},t} + \nu_{\mathrm{res},t} \right) + \varsigma_{\mathrm{res},t} + \xi_t \ge 0, \\ \mu_{\mathrm{res},t}, \nu_{\mathrm{res},t}, \varsigma_{\mathrm{res},t}, \zeta_t \ge 0, \end{cases} \end{aligned} \tag{19}$$

where $x_{\mathrm{res},t}, y_{\mathrm{res},t}, \alpha_{\mathrm{res},t}, \beta_t$ and $\mu_{\mathrm{res},t}, \nu_{\mathrm{res},t}, \varsigma_{\mathrm{res},t}, \zeta_t$ are the dual constraint variable. RL% indicates the spinning reserve capacity ratio of the system.

After conversion by using robust theory, the day-ahead robust scheduling optimization model is converted into an MILP model, which is solved, and the effects of different energy storage devices on the system are considered.

4. Simulation Analysis

In this paper, an EHG-IES park is used as a simulation object for analysis under the uncertainty of wind power and PV output. The system includes EVs, HS, wind power, PV, electrical loads, and heating loads. The parameters and predicted data for each equipment part are shown in Tables 1 and 2 and Figure 2 [29]. The rest of the parameters are given in [30].

4.1. Analysis of Scheduling Results under Different Methods. The established models are analyzed separately by using the proposed method and the SO considering the uncertainty of

Table 1: Equipment parameters.

Parameters	Parameter value
$P_{MT1,min}, P_{MT2,min}, P_{MT3,min}$/kW	15, 15, 15
$P_{MT1,max}, P_{MT2,max}, P_{MT3,max}$/kW	600, 400, 200
$\eta_{MT}, \eta_L, \eta_h$	0.9, 0.02, 0.93
$C_{OP,h}$	1.5
$P_{MT1,up}, P_{MT2,up}, P_{MT3,up}$/kW	220, 160, 80
$P_{MT1,down}, P_{MT2,down}, P_{MT3,down}$/kW	220, 160, 80
$\phi_{MT1}, \phi_{MT2}, \phi_{MT3}$	2.64, 2.7, 0.6
$\varphi_{MT1}, \varphi_{MT2}, \varphi_{MT3}$	66.2, 50, 12

Table 2: Timeshare tariffs.

Tariff type	Electricity price (¥/kWh)	Time period
Valley	0.45	00:00–07:00 22:00–24:00
Usual period	0.73	12:00–18:00
Peak	1.21	07:00–12:00 18:00–22:00

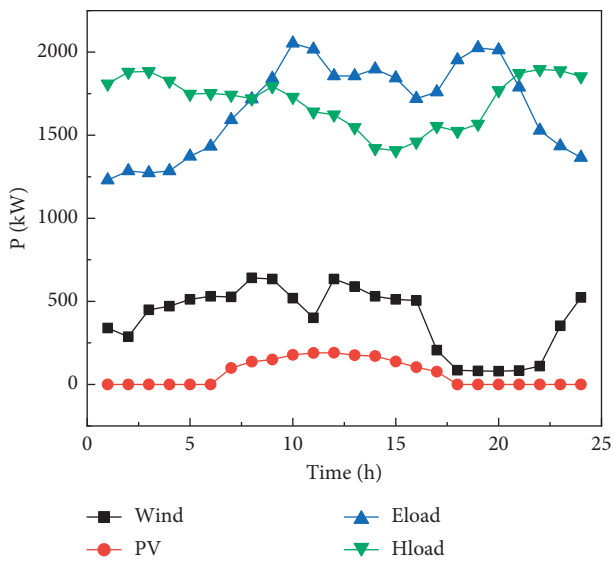

Figure 2: Wind, PV, and load power.

wind power and PV output, and the obtained results are shown in Table 3.

The results calculated using the method in this paper with different robust parameters, SO, and the deterministic model are shown in Table 3. In the abovementioned methods, the calculations consider both EVs and HS. Different degrees of the uncertainty of wind power and PV output are reflected by robust parameters. In the case of robust parameters of 10% and 20% [31, 32], the larger the selection of robust parameters, the higher the cost required. Moreover, as the value of the robust parameter increases, the cost shows an increasing trend as the operating cost of the equipment. However, power purchase costs are reduced instead, and the total system cost is proportional to the robust parameters. However, the system cost will be further increased if the robustness needs to be considered for larger cases. For robust parameters of 20% and 10%, the economic cost is 1.016% and 1.041% lower than that of the SO. Also, for robust parameters of 20% and 10%, the economic cost is 1.914% and 1.939% lower than that of the deterministic model. Deterministic models have no consideration of the uncertainty of RES output, which requires higher costs to cope with scheduling problems. There is a relationship between economy and robustness. In contrast to SO, SO utilizes MC methods for scenario generation to achieve an uncertain description of wind power and PV output. Compared with the robust optimization method in this paper, the cost is higher, which verifies the accuracy and economy of the suggested method. The results in Table 3 show that the proposed method can improve the economy of the system and can better address the uncertainty of the RES output.

The results are analyzed with the robustness parameter of 20% in the method of this paper. The power output of the unit and energy storage equipment obtained in this case is shown in Figures 3 and 4.

In Figures 3 and 4, PGB is the GB output power. P_{eb} denotes the EB output power. P_{grid} is the power purchased from the upper grid. H_{hsdis} and H_{hscha} represent the discharge and storage power of HS. P_{esdis} and P_{escha} represent the discharging and charging power of EVs.

According to Figures 3 and 4, it can be concluded that, during 0:00–07:00, the load is also at the valley when the tariff is low. Also, the wind power and PV output gradually increase with the increase of time. At this time, the electrical load is mainly met by wind power, PV and the purchase of electricity from the upper grid, and charging of EVs. Also, the heating load is not in the valley at this time, mainly through the GB and EB to meet the requirements of the heating load. The HS can store heat. During the 07:00–12:00 electricity price peak hours, the electric load demand gradually rises, and the heating load demand has a decreasing trend. The output of the three MT units starts to increase. At this time, electricity prices are higher, EVs' electricity is discharged, and less power is purchased from the upper grid to meet the electrical demand. Compared to low electricity prices, the heating load demand is reduced and the excess heat energy is stored by HS. During the 12:00–18:00 period, the electrical and heating loads are reduced, and the electrical load is mainly carried by the power purchased from the upper grid and EB. The heating load is mainly carried by EB. The heat energy price is low, and HS performs heat storage. During the evening peak hours of 18:00–22:00, wind power output is lower than in the morning peak hours. The three MT units increase their output and simultaneously purchase power from the upper grid and use EB to meet it. The EB converts excess electrical energy into heat energy for the heat load and the needs of the HS. The role of different energy storage devices varies under different load requirements. EVs discharge at peak load times, thereby reducing the peak load. EVs charge during load valleys to increase the load value. Also, for heat storage devices, they are mainly discharged at night. This is because people are at rest time at night and need to release heat energy.

Table 3: Obtained results of different methods.

Method	Robust parameters (%)	Power purchase costs (¥)	Operating costs (¥)	Total cost (¥)
Method of this paper	10	16266.0100	35613.1486	51879.1586
	20	16239.3700	35652.9809	51892.3509
SO	—	16893.7805	35531.4256	52425.2061
Deterministic model	—	16213.3600	36691.6152	52904.9752

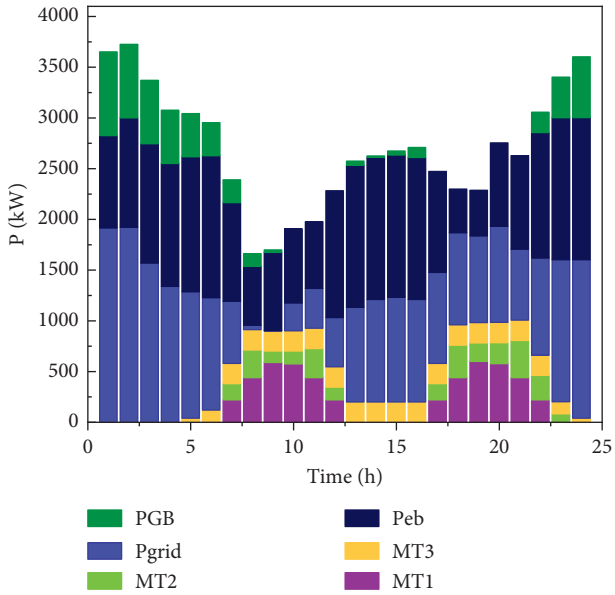

Figure 3: Unit power output.

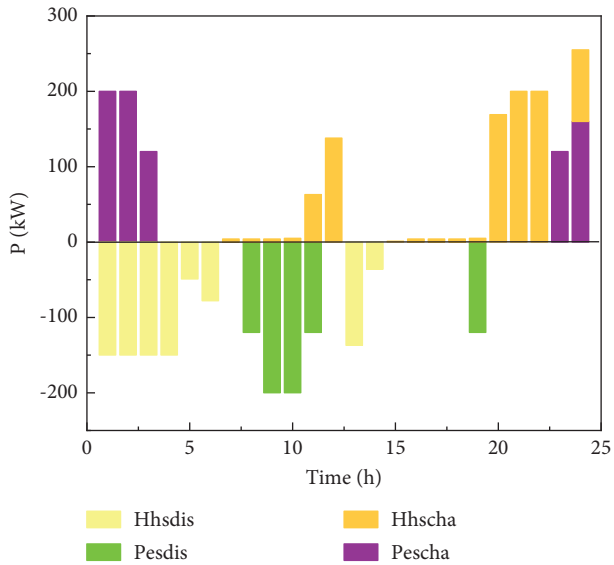

Figure 4: Energy storage output.

4.2. Comparative Analysis of Different Energy Storage Devices. To analyze the impact of different energy storage devices, the case containing both EVs and HS (C1) and the case containing only EVs (C2) are considered. Also, we consider the results of EVs at different charging and discharging efficiencies for comparison. The charge/discharge efficiency of EVs is set to 0.9 considering EVs and HS (C3). The results obtained from the comparative analysis using the proposed method with a robust parameter of 20% are shown in Table 4.

The results in Table 4 show that the total costs do not differ much in the two different cases. The negative signs in Figures 5–7 are used to distinguish the comparison and do not indicate the magnitude of the values. In the case of C1, the upper grid power purchase cost is slightly higher than C2. The presence of both is more economical than the case of a single energy storage device and improves energy efficiency. In the two different cases, the main analysis of the unit output is performed, focusing on the output of MT and EB. In C1 and C3, a comparative analysis is performed considering different charging and discharging efficiencies. There is a relationship between charging and discharging efficiency and total cost. The higher the charging and discharging efficiency, the lower the total cost required. In C1 and C3, the output of EBs are shown in Figure 6. As can be seen from Figure 6, the EB output is also lower at lower charge/discharge efficiencies. According to the simulation results, it can be obtained that the higher charging and discharging efficiency of EVs can reduce the total cost of scheduling. Therefore, the future development needs to focus on improving the charging and discharging efficiency of energy storage battery.

The output of MT1 and EB units is compared and analyzed under different conditions. The output of EB is basically the same in C1 and C2; therefore, only the results in C1 and C2 are analyzed for comparison. We can get that the main difference in MT1 unit output is in the first peak period when the electric load gradually increases and the heat load slightly decreases from Figure 5. In the period 05:00–08:00, the output of the MT1 unit in the C2 case is slightly smaller than that in the C1 case. In the case of C1, part of the load is supplied by the HS, but the uncertainty of wind power and PV output needs to be considered. In the rest of the period, the MT unit output is more or less the same. The main difference is in the 00:00–08:00 and 19:00–22:00 time periods for the EB output in Figure 6. Between 00:00–05:00, the EB output is greater in the C2 than in the C1. Moreover, between 05:00–08:00, the C1 output of EB is greater than the C2 output. During the evening peak period, the output power under C1 is greater. Between 00:00–05:00, the heating load demand is high, and the HS in C1 exerts heat to meet the heating load demand. When the HS is not included in C2, EB increases the output to meet it. During 05:00–08:00, the heating load demand decreases, the HS is not required for heat storage, and the EB output decreases. During the evening peak, the heat energy generated by GB and EB is

Table 4: Scheduling results under different energy storage devices.

Case	Upper grid power purchase costs (¥)	Operating costs (¥)	Total cost (¥)
C1	16239.3700	35652.9809	51892.3509
C2	15994.8100	36924.1683	52918.9783
C3	16283.0000	35618.3710	51901.3710

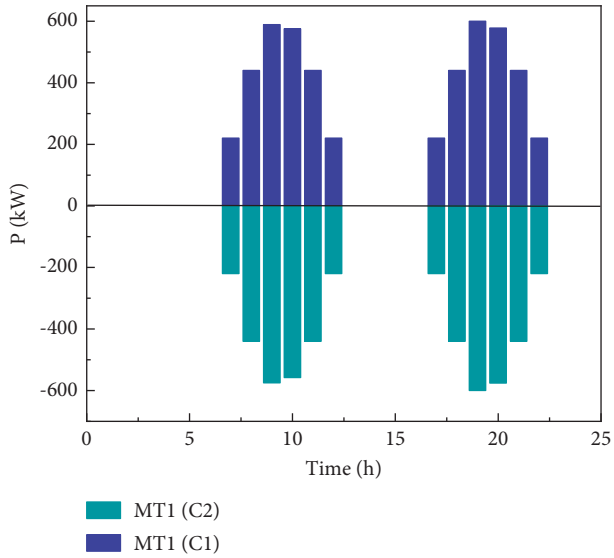

Figure 5: MT1 unit power output.

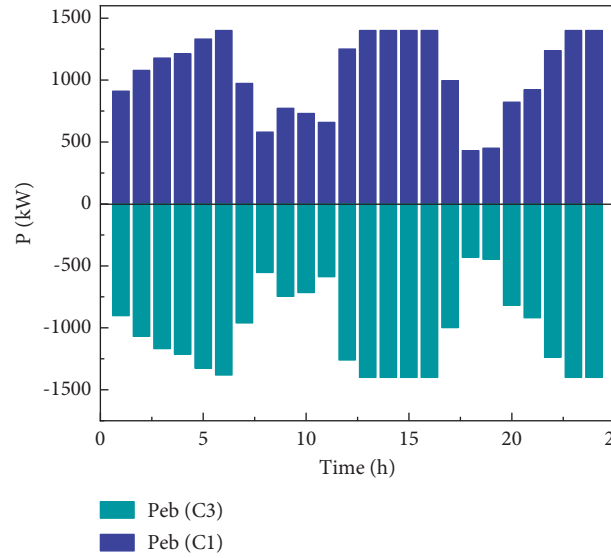

Figure 7: EB power output (C1 and C3).

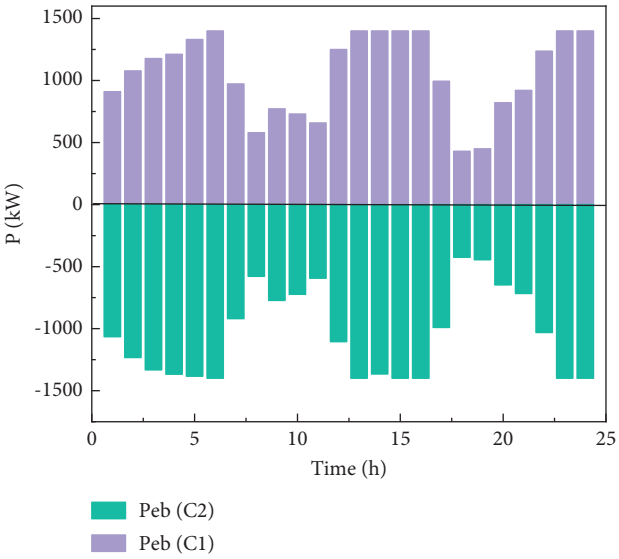

Figure 6: EB power output (C1 and C2).

sufficient to meet the load demand. However, the excess heat energy is not utilized because there is no HS, which is why EB output is larger in the case of C1 than in C2. HS stores excess heat energy, which can improve energy utilization, reduce energy waste, and achieve energy sustainability. In summary, in the absence of HS, the economic costs are increased to a certain extent, and the energy utilization rate is reduced, making some energy underutilized. During the night time, the heat storage unit produces more power. Therefore, different energy storage devices need to work better together at different times of the day to improve energy utilization.

5. Conclusions

For the EHG-IES containing the uncertainty of wind power and PV output, the role of different energy storage devices is considered, and the uncertainty of wind power and PV output is described by the set of maximum uncertainty containing addition. The day-ahead robust optimization model of EHG-IES is established. The following conclusions are obtained:

(1) The uncertainty of RES output in the EHG-IES is represented by the set of maximum uncertainty containing addition. Then, the robust optimization day-ahead model of EHG-IES considering EVs and HS is established. The charging and discharging efficiency of EVs have a large impact on scheduling optimization. The higher the charging and discharging efficiency, the lower the scheduling cost.

(2) Different robust parameters are set for the uncertainty of wind power and PV output to achieve the control of the robustness of the system. Also, as the robust parameters are chosen larger, the total cost required for the system is more and the results obtained are more conservative.

(3) Comparative analysis of the role of different energy storage devices in the EHG-IES is presented. In the case of considering both EVs and HS, it can improve

the economy and energy utilization. Collaborative and optimal scheduling of HS and EVs can improve energy efficiency.

The next research will investigate the uncertainty of source-load dual-side and low-carbon economic scheduling to improve the system economy and energy utilization.

Data Availability

The data used to support the findings of this study are available from the corresponding author upon request.

Conflicts of Interest

The authors declare no conflicts of interest.

Acknowledgments

This research was funded by the Program of the Natural Science Foundation of Hunan Province, (Grant no. 2019jj40200), the Program of the Natural Science Foundation of Hunan Province, (Grant no. 2019jj6002), the Research Foundation of Education Bureau of Hunan Province, China (Grant no. 19B393), the Scientific and Technological Innovation and Development Project of Changde District (Grant no. 2020C083), and the Science and Technology Innovation Program of Hunan Province (Grant no. 2021GK2010).

References

[1] J. Li, D. Li, Y. Zheng, Y. Yao, and Y. Tang, "Unified modeling of regionally integrated energy system and application to optimization," *International Journal of Electrical Power and Energy Systems*, vol. 134, Article ID 107377, 2022.

[2] P. Li, Z. Wang, H. Liu, J. Wang, T. Guo, and Y. Yin, "Bi-level optimal configuration strategy of community integrated energy system with coordinated planning and operation," *Energy*, vol. 236, Article ID 121539, 2021.

[3] Y. Jiang and L. Guo, "Research on wind power accommodation for an electricity-heat-gas integrated microgrid system with power-to-gas," *IEEE Access*, vol. 7, pp. 87118–87126, 2019.

[4] D. Xu, Q. Wu, B. Zhou, C. Li, L. Bai, and S. Huang, "Distributed multi-energy operation of coupled electricity, heating, and natural gas networks," *IEEE Transactions on Sustainable Energy*, vol. 11, pp. 2457–2469, 2019.

[5] Z. Wang, J. Hu, and B. Liu, "Stochastic optimal dispatching strategy of electricity-hydrogen-gas-heat integrated energy system based on improved spectral clustering method," *International Journal of Electrical Power and Energy Systems*, vol. 3, p. 126, 2021.

[6] Y. Li, Y. Zou, Y. Tan et al., "Optimal stochastic operation of integrated low-carbon electric power, natural gas, and heat delivery system," *IEEE Transactions on Sustainable Energy*, vol. 9, no. 1, pp. 273–283, 2018.

[7] A. A. Eladl, M. I. El-Afifi, M. A. Saeed, and M. M. El-Saadawi, "Optimal operation of energy hubs integrated with renewable energy sources and storage devices considering CO_2 emissions," *International Journal of Electrical Power and Energy Systems*, vol. 117, Article ID 105719, 2020.

[8] E. Shahrabi, S. M. Hakimi, A. Hasankhani, G. Derakhshan, and B. Abdi, "Developing optimal energy management of energy hub in the presence of stochastic renewable energy resources," *Sustainable Energy, Grids and Networks*, vol. 26, Article ID 100428, 2021.

[9] Z. Yuan, S. He, A. a. Alizadeh, S. Nojavan, and K. Jermsittiparsert, "Probabilistic scheduling of power-to-gas storage system in renewable energy hub integrated with demand response program," *Journal of Energy Storage*, vol. 29, Article ID 101393, 2020.

[10] S. M. Nosratabadi, M. Jahandide, and J. M. Guerrero, "Robust scenario-based concept for stochastic energy management of an energy hub contains intelligent parking lot considering convexity principle of CHP nonlinear model with triple operational zones," *Sustainable Cities and Society*, vol. 68, Article ID 102795, 2021.

[11] Y. Cao, W. Wei, J. Wang, S. Mei, M. Shafie-Khah, and J. P. S. Catalao, "Capacity planning of energy hub in multi-carrier energy networks: a data-driven robust stochastic programming approach," *IEEE Transactions on Sustainable Energy*, vol. 11, no. 1, pp. 3–14, 2020.

[12] S. Geng, M. Vrakopoulou, and I. A. Hiskens, "Optimal capacity design and operation of energy hub systems," *Proceedings of the IEEE*, vol. 108, no. 9, pp. 1475–1495, 2020.

[13] E. A. Martinez Cesena and P. Mancarella, "Energy systems integration in smart districts: robust optimisation of multi-energy flows in integrated electricity, heat and gas networks," *IEEE Transactions on Smart Grid*, vol. 10, no. 1, pp. 1122–1131, 2019.

[14] P. Li, Z. Wang, N. Wang et al., "Stochastic robust optimal operation of community integrated energy system based on integrated demand response," *International Journal of Electrical Power and Energy Systems*, vol. 128, Article ID 106735, 2021.

[15] S. M. Nosratabadi, M. Jahandide, and R. K. Nejad, "Simultaneous planning of energy carriers by employing efficient storages within main and auxiliary energy hubs via a comprehensive MILP modeling in distribution network," *Journal of Energy Storage*, vol. 30, Article ID 101585, 2020.

[16] K. Zhang, B. Zhou, C. Li et al., "Dynamic modeling and coordinated multi-energy management for a sustainable biogas-dominated energy hub," *Energy*, vol. 220, Article ID 119640, 2021.

[17] G. Zhang, Z. Shen, and L. Wang, "Online energy management for microgrids with CHP co-generation and energy storage," *IEEE Transactions on Control Systems Technology*, vol. 28, no. 2, pp. 533–541, 2020.

[18] H. Fan, Q. Yuan, S. Xia, J. Lu, and Z. Li, "Optimally coordinated expansion planning of coupled electricity, heat and natural gas infrastructure for multi-energy system," *IEEE Access*, vol. 8, pp. 91139–91149, 2020.

[19] D. Xie, A. Chen, C. Gu, and J. Tai, "Time-domain modeling of grid-connected CHP for its interaction with the power grid," *IEEE Transactions on Power Systems*, vol. 33, no. 6, pp. 6430–6440, 2018.

[20] Q. Wang, J. Liu, Y. Hu, and X. Zhang, "Optimal operation strategy of multi-energy complementary distributed CCHP system and its application on commercial building," *IEEE Access*, vol. 7, pp. 127839–127849, 2018.

[21] Z. Li, Y. Xu, S. Fang, Y. Wang, and X. Zheng, "Multiobjective coordinated energy dispatch and voyage scheduling for a multienergy ship microgrid," *IEEE Transactions on Industry Applications*, vol. 56, no. 2, pp. 989–999, 2020.

[22] X. Guo, S. Han, L. Qin, L. Sun, W. Wu, and M. Liao, "Operation optimization of integrated energy system from the

perspective of sustainable development," *IEEE Access*, vol. 8, pp. 65148–65154, 2020.

[23] Y. Ma, H. Wang, F. Hong et al., "Modeling and optimization of combined heat and power with power-to-gas and carbon capture system in integrated energy system," *Energy*, vol. 236, Article ID 121392, 2021.

[24] W. Gan, M. Yan, W. Yao et al., "Decentralized computation method for robust operation of multi-area joint regional-district integrated energy systems with uncertain wind power," *Applied Energy*, vol. 298, Article ID 117280, 2021.

[25] L. Lundström and F. Wallin, "Heat demand profiles of energy conservation measures in buildings and their impact on a district heating system," *Applied Energy*, vol. 161, pp. 290–299, 2016.

[26] W. Gu, Z. Wang, and Z. Wu, "An online optimal dispatch schedule for CCHP microgrids based on model predictive control," *IEEE Transactions on Smart Grid*, vol. 8, no. 5, pp. 2332–2342, 2016.

[27] X. Xu, H. Jia, and H. D. Chiang, "Dynamic modeling and interaction of hybrid natural gas and electricity supply system in microgrid," *IEEE Transactions on Power Systems*, vol. 30, no. 3, pp. 1212–1221, 2014.

[28] Z. Liu, Q. Wu, S. Huang, L. Wang, M. Shahidehpour, and Y. Xue, "Optimal day-ahead charging scheduling of electric vehicles through an aggregative game model," *IEEE Transactions on Smart Grid*, vol. 9, no. 5, pp. 5173–5184, 2018.

[29] Capstone Turbine Corporation: Capstone C200 Micoturbine Technical Reference, 2009, https://interstatepower.us/Capstone%20Document%20Library/Technica1%20Reference/410066C_C200_Tech_Ref.pdf.

[30] S. Cheng, T. Huang, and R. Wai, "Multi-time-scale optimal scheduling of CCHP microgrid with ice-storage air-conditioning," *Automation of Electric Power Systems*, vol. 43, no. 5, pp. 30–38, 2019.

[31] J. J. Miettinen and H. Holttinen, "Characteristics of day-ahead wind power forecast errors in Nordic countries and benefits of aggregation," *Wind Energy*, vol. 20, no. 6, pp. 959–972, 2017.

[32] A. Dolara, S. Leva, and G. Manzolini, "Comparison of different physical models for PV power output prediction," *Solar Energy*, vol. 119, pp. 83–99, 2015.